Coordinated regulation of skeletal muscle mass and metabolic plasticity during recovery from disuse

THE FASEB JOURNAL • RESEARCH • www.fasebj.org

Coordinated regulation of skeletal muscle mass and metabolic plasticity during recovery from disuse

Anita Kneppers,* Pieter Leermakers,* Nicholas Pansters,* Evelien Backx,† Harry Gosker,* Luc van Loon,† Annemie Schols,* Ramon Langen,*,[1] and Lex Verdijk†,[1,2]

*Department of Respiratory Medicine and †Department of Human Biology, School of Nutrition and Translational Research in Metabolism (NUTRIM), Maastricht University Medical Centre+, Maastricht, The Netherlands

ABSTRACT: Skeletal muscle regeneration after disuse is essential for muscle maintenance and involves the regulation of both mass- and metabolic plasticity–related processes. However, the relation between these processes during recovery from disuse remains unclear. In this study, we explored the potential interrelationship between the molecular regulation of muscle mass and oxidative metabolism during recovery from disuse. Molecular profiles were measured in biopsies from the vastus lateralis of healthy men after 1-leg cast immobilization and after 1 wk reloading, and in mouse gastrocnemius obtained before and after hindlimb suspension and during reloading (RL-1, -2, -3, -5, and -8 d). Cluster analysis of the human recovery response revealed correlations between myogenesis and autophagy markers in 2 clusters, which were distinguished by the presence of markers of early myogenesis, autophagosome formation, and mitochondrial turnover *vs.* markers of late myogenesis, autophagy initiation, and mitochondrial mass. In line with these findings, an early transient increase in B-cell lymphoma-2 interacting protein-3 and sequestosome-1 protein, and GABA type A receptor-associated protein like-1 protein and mRNA and a late increase in myomaker and myosin heavy chain-8 mRNA, microtubule-associated protein 1 light chain 3-II:I ratio, and FUN14 domain-containing-1 mRNA and protein were observed in mice. In summary, the regulatory profiles of protein, mitochondrial, and myonuclear turnover are correlated and temporally associated, suggesting a coordinated regulation of muscle mass– and oxidative metabolism–related processes during recovery from disuse.—Kneppers, A., Leermakers, P., Pansters, N., Backx, E., Gosker, H., van Loon, L., Schols, A., Langen, R., Verdijk, L. Coordinated regulation of skeletal muscle mass and metabolic plasticity during recovery from disuse. FASEB J. 33, 1288–1298 (2019). www.fasebj.org

KEY WORDS: remobilization · remodeling · protein turnover · myogenesis · mitophagy

Skeletal muscles are essential to generate the forces for postural support and physical function. Furthermore, representing half of the body mass and being highly metabolically active, skeletal muscle tissue is an important site for control of metabolism (1). These functions are supported by the muscles' biochemical and morphologic makeup, which are tightly regulated and can rapidly adapt to alterations in mechanical and metabolic demands—referred to as skeletal muscle plasticity.

Muscle disuse results from low skeletal muscle mechanical loading, such as occurs with bed rest during hospitalization after surgery or acute illness, with immobilization after a fracture, and with certain chronic diseases. It is well established that disuse leads to a reduction of skeletal muscle strength (2) and mass (2, 3), which results from a negative balance in muscle protein turnover (2, 4). In addition, disuse affects muscle quality, including a transition from a slow to fast fiber type (5–7), a shift from fat oxidation toward glycolysis (8), a decrease in mitochondrial mass and function (9–12), and a reduction in vascularization (13).

The above-mentioned qualitative alterations in response to disuse collectively reduce the capacity for oxidative metabolism. It has been suggested that these metabolic alterations represent an adaptation to a decreased energy requirement resulting from a reduction in the level of protein turnover upon disuse (8). On the other hand, a study showed that the inhibition of disuse-induced

ABBREVIATIONS: 1-RM, one-repetition maximum; BECN, beclin; BL, baseline; BNIP3, BCL2 interacting protein 3; CSA, cross-sectional area; FUNDC1, FUN14 domain containing 1; GABARAPL1, GABA type A receptor associated protein like 1; MAP1LC3B, microtubule associated protein 1 light chain 3 β; MSTN, myostatin; MYH, myosin heavy chain; MYMK, myomaker; MYOG, myogenin; OPTN, optineurin; PAX, paired box; PINK1, PTEN-induced putative kinase 1; PRKN, parkin RBR E3 ubiquitin protein ligase; RL, reloading; SC, satellite cell; SQSTM1, sequestosome 1; TBST, Tris-buffered saline with Tween 20; UL, unloading; ULK1, unc-51 like autophagy activating kinase 1

[1] These authors contributed equally to this work.

[2] Correspondence: Department of Human Biology, Maastricht University, PO Box 616, 6200 MD Maastricht, The Netherlands. E-mail: lex.verdijk@maastrichtuniversity.nl

doi: 10.1096/fj.201701403RRR

This article includes supplemental data. Please visit *http://www.fasebj.org* to obtain this information.

0892-6638/19/0033-1288 © FASEB

mitochondrial alterations prevents the loss of muscle mass (12). These findings indicate that muscle disuse–induced mass and metabolic alterations are highly interdependent.

Although disuse-induced alterations in skeletal muscle mass and function may be part of a normal physiologic response, the negative implications of muscle disuse atrophy for general health, quality of life (14), and even survival (15–17) have been clearly demonstrated. Both nutritional interventions and exercise mimetics have been used to prevent muscle disuse atrophy, but none serve as a complete substitute for the mechanical and metabolic stimulation during normal muscle use (18–22). Nevertheless, in otherwise healthy individuals, a normalization of muscle mass and function occurs upon reloading after disuse (23, 24). However, the negative consequences of disuse may persist when muscle regeneration is impaired, as occurs in elderly (25–27) and chronically ill persons (28). To identify and target factors that hamper skeletal muscle recovery during resumed physical activity after disuse in such persons, a better understanding of the molecular alterations driving skeletal muscle plasticity during reloading-induced recovery is imperative.

In contrast to the wealth of data on the molecular alterations during skeletal muscle disuse in both humans and animals, insight into the molecular response to reloading to induce skeletal muscle regeneration is less abundant and depends mainly on data from studies in rodents. From these studies, it is clear that protein synthesis signaling related to the control of mRNA translation is increased upon reloading after disuse (27, 29, 30) and that markers of the ubiquitin proteasome system (UPS) return to baseline levels during reloading (24, 30). Rather than a passive normalization of the protein turnover balance, several studies suggest a transient activation of protein degradation signaling during reloading-induced recovery, particularly of the autophagy-lysosome pathway (24, 27, 31, 32). In addition, myogenesis seems to be activated during skeletal muscle reloading (4, 30, 33).

These reloading-induced molecular alterations are also implicated in intrinsic remodeling of skeletal muscle. Indeed, metabolic alterations take place upon skeletal muscle reloading, including an activation of processes that regulate mitochondrial biogenesis and function (32, 34, 35) and an increase in mitochondrial mass (32, 34). Similar to the interdependency of mass and metabolic alterations upon muscle disuse, these processes may be linked during reloading-induced recovery. However, such a potential relation is largely understudied. In the present study, we therefore sought to provide insight in the interrelationship between the regulation of muscle mass and muscle metabolic plasticity during recovery from disuse. A better understanding of these relations is essential for the identification of the molecular origin, and subsequent treatment, of impaired remobilization-induced skeletal muscle recovery in the elderly and chronically ill. We explored these relations by measuring a selected set of indicators and molecular regulators and mediators of muscle mass– and oxidative metabolism–related processes and studied their interrelationship during reloading-induced recovery after disuse in both humans and rodents.

MATERIALS AND METHODS

Subjects, study design, and measurements

Skeletal muscle molecular profiles of 14 healthy young men (age, 23 ± 1 yr; body mass index, 22.9 ± 0.6 kg/m^2) who participated in a double-blind, randomized, placebo-controlled intervention trial (*www.clinicaltrials.gov*; NCT01894737) were analyzed. Written informed consent was obtained from all subjects, and the study was approved by the Maastricht University Medical Center+ (Maastricht, The Netherlands) ethics review board (13-3-023) and performed in accordance with the Declaration of Helsinki. The study design and primary data were published previously (36). In brief, participants were subjected to 7 d of 1-leg immobilization by means of a full leg cast [unloading (UL)], followed by 7 d of remobilization [reloading (RL)]. Subjects were asked to maintain habitual dietary intake and refrain from any heavy physical exercise during the entire intervention period. Their compliance was checked and confirmed by dietary intake records and activity journals. Furthermore, the subjects consumed standardized meals the evening before all test days. Needle biopsies from the vastus lateralis of the casted leg were taken after an overnight fast after UL and again after RL. Samples were frozen in liquid nitrogen and stored at −80°C until further analysis. Furthermore, muscle mass, measured by cross-sectional area (CSA) was assessed by a computed tomographic scan of the upper legs, muscle strength was assessed with a 1-repetition maximum (1-RM) knee extension test, and body weight was measured with a digital scale. None of the subjects performed progressive resistance-type exercise training or took creatine supplements or any medication that would interfere with muscle metabolism in the 6 mo before the study.

Only subjects with a complete set of available muscle biopsies were included in the current subanalysis (n = 14), of whom 5 received placebo and 9 received creatine supplementation. Based on an increase of <10 mM/kg in muscle total creatine content (36), 4 subjects were considered nonresponders to creatine loading. Furthermore, creatine supplementation did not have any impact on muscle disuse or subsequent recovery (36).

Animals and study design

The animal study was approved by the Institutional Animal Care Committee of Maastricht University (DEC-2009-074). The study design has been published (30, 34). In the current subanalysis, only the control (*i.e.*, GSK-3β$^{fl/fl}$ MLC1f-Cre$^{-/-}$) animals were used. In brief, 13-wk-old male C57/Bl6 mice were housed in a temperature-controlled room (21–22°C) with a 12–12 h light–dark cycle and standard chow pellets and water *ad libitum*. Mice were subjected to either no experimental procedure (baseline, BL; n = 9), 14 d of muscle UL by hindlimb suspension (UL, n = 8), or 1, 2, 3, 5, or 8 d of RL after hindlimb suspension (n = 8 per time point). Mice were euthanized at each time point by injection with pentobarbital sodium, and hindlimb muscles were excised with standardized dissection methods. Muscles were cleaned of excess fat and connective tissue, pair weighed on an analytical scale, and snap frozen in liquid nitrogen (biochemical analyses) or embedded in Tissue-Tek optimal cutting temperature compound (Sakura Finetek, Zoeterwolde, The Netherlands) and frozen in melting isopentane (histochemical analyses). Samples were stored at −80°C until further analysis. The gastrocnemius was used for protein and mRNA analyses, as its response to hindlimb UL is pronounced and well characterized in studies (37–39). Furthermore, it has a fiber type composition and distribution that is representative of many muscles in the hindlimb and is similar to the fiber type composition observed in the human vastus lateralis.

Protein isolation and Western blot analysis

For protein analysis, frozen mouse gastrocnemius was powdered and lysed in a whole-cell lysis buffer (50 mM Tris, 150 mM NaCl, 10% glycerol, 0.5% Nonidet P40, 1 mM EDTA, 500 μM Na_3VO_4, 500 μM NaF, 100 μM β-glycerophosphate, 100 μM $Na_4P_2O_7$, 1 mM DTT, 10 μg/ml leupeptin, and 1% aprotinin) for 1 h on a tube rotator at 4°C, followed by 30 min of centrifugation at 14,000 *g* at 4°C. Lysates were aliquoted in sample buffer [0.25 M Tris-HCl, 8% (w/v) SDS, 40% (v/v) glycerol, 0.4 M DTT, and 0.02% (w/v) bromophenol blue], boiled for 5 min at 95°C, and stored at −80°C. Human vastus lateralis biopsies were homogenized in lysis buffer (20 mM Tris-HCl, 1% Nonidet P40, 5 mM EDTA, 2 mM Na_3VO_4, 100 mM NaF, 10 mM $Na_4P_2O_7$, 10 μg/ml leupeptin, 10 μg/ml aprotinin, 3 mM benzamidine, and 1 mM PMSF) using an Ultra-Turrax (IKA Works, Wilmington, NC, USA). Lysates were centrifuged for 10 min at 10,000 *g* at 4°C. Lysates were aliquoted in sample buffer [0.35 M Tris-HCl, 10% (w/v) SDS, 30% (v/v) glycerol, 0.6 M DTT, and 0.02% bromophenol blue], boiled for 5 min at 100°C, and stored at −80°C. Total protein concentration was determined with the Pierce BCA Protein Assay Kit (Thermo Fisher Scientific, Waltham, MA, USA), according to the manufacturer's instructions.

Ten micrograms protein was separated on a Criterion XT Precast Bis-Tris Gel (Bio-Rad, Hercules, CA, USA) in XT-3-(*N*-morpholino)propanesulfonic acid or XT-2-[*N*-morpholino]ethanesulfonic acid running buffer (Bio-Rad) by gel electrophoresis. Proteins were transferred to a 0.45 μm nitrocellulose membrane (Bio-Rad) by electroblotting at 100 V for 60 min in transfer buffer [25 mM Tris, 192 mM glycine, 20% (v/v) methanol]. For total protein detection, membranes were stained with PonceauS solution (0.2% PonceauS in 1% acetic acid; MilliporeSigma, Burlington, MA, USA) for 3–5 min, washed in double-distilled H_2O for 30 s on a shaker, and imaged with the Amersham imager 600RGB (GE Healthcare, Chicago, IL, USA). The membranes were blocked for 1 h at room temperature in Tris-buffered saline with Tween 20 [TBST; 20 mM Tris, 137 mM NaCl, 0.1% (v/v) Tween 20 (pH 7.6)] containing 5% (w/v) nonfat dry milk (Campina, Eindhoven, The Netherlands). The membranes were washed in TBST, followed by overnight incubation at 4°C with primary antibody diluted in TBST with 3% bovine serum albumin (Supplemental Table S1). After a wash in TBST, membranes were incubated with a peroxidase-conjugated secondary antibody solution (Vector Laboratories, Burlingame, CA, USA) for 1 h at room temperature, and targets were visualized by chemiluminescence (Supersignal West PICO or FEMTO Chemiluminescent substrate; Thermo Fisher Scientific), according to the manufacturer's instructions, and detected with the Amersham Imager 600RGB. Signals were quantified with Image Quant TL software (GE Healthcare). Samples from each group were distributed within and between blots, to allow for correction of between-session variation (40), and protein expression and phosphorylation levels were corrected for protein loading assessed by PonceauS.

RNA isolation and RT-qPCR

For RNA analysis, powdered mouse gastrocnemius was lysed in RLT solution containing 1% 2-ME. Total RNA was extracted using an on-column RNA isolation kit (Qiagen, Hilden, Germany) according to the manufacturer's instructions and stored at −80°C. Human vastus lateralis biopsies were lysed in Trizol (Thermo Fisher Scientific). Total RNA was isolated by phenol-chloroform extraction and subsequent precipitation from the aqueous phase with glycogen-containing isopropanol. RNA was reconstituted in nuclease-free H_2O and stored at −80°C.

RNA concentration was determined with a spectrophotometer (Nanodrop ND-1000 UV-Vis; Thermo Fisher Scientific). RNA (400 ng/sample) was reverse transcribed into cDNA with a Transcriptor cDNA synthesis kit (Roche, Basel Switzerland), according to the manufacturer's instructions. Primers were designed based on Ensemble transcript sequences and ordered from MilliporeSigma, with primer details shown in Supplemental Table S2. qPCR reactions contained Sensimix Sybr Rox (GC Biotech, Alphen aan den Rijn, The Netherlands) and primer mix and were run in a 384-well white opaque plate (Roche Diagnostics, Indianapolis, IN, USA) on a LightCycler 480 system (Roche Diagnostics). Melting curves were analyzed to verify specificity of the amplification, and relative quantity of the targets was assessed by LinRegPCR software (v.2014.8; *http://www.hartfaalcentrum.nl*) (Heart Failure Research Centre, Amsterdam, The Netherlands). Study-specific reference genes (Supplemental Table S2) were used to calculate a GeNorm correction factor (*https://genorm.cmgg.be/*), which was used to normalize expression levels of the target genes.

Immunohistochemistry

OCT-embedded, frozen mouse gastrocnemius was cut (7 μm), defrosted, and air dried at room temperature. Tissue was fixed with 4% paraformaldehyde and permeabilized with 0.2% Triton X-100 in PBS. Subsequently, samples were treated for 60 min with 3% H_2O_2, blocked for 60 min in blocking solution [5% (v/v) goat serum, 2% (w/v) bovine serum albumin, 1:40 mouse-on-mouse blocking reagent (MOM; Vector Laboratories)] at room temperature, and incubated overnight at 4°C with primary antibodies directed against laminin and paired box (PAX)-7 (1:250) (Supplemental Table S1). Samples were incubated in horseradish peroxidase–conjugated streptavidin and goat anti-rabbit 555 (1:200) for 60 min at room temperature and subsequently for 7 min in tyramide working solution and reaction stop reagent, according to the manufacturer's protocol (Tyramide SuperBoost Kit; Thermo Fisher Scientific). Nuclei were stained with DAPI, after which cover slips were mounted with Mowiol (MilliporeSigma). After staining, images were digitally captured with fluorescence microscopy (Olympus IX-81; Olympus, Hamburg, Germany) connected to a digital camera (EXi Aqua; QImaging, Surrey, BC, Canada) at ×400 magnification. Image processing and quantitative analyses were performed with ImageJ (National Institutes of Health, Bethesda, MD, USA).

Laminin staining was used to determine the cell borders. Within each image, the mean fiber CSA, the number of myonuclei per fiber, and the mean fiber CSA per nucleus were quantified. Satellite cells (SCs) were manually counted and were defined as $PAX7^+$ nuclei located within the basal lamina.

Data analysis and statistics

To address the relation between alterations in skeletal muscle mass– and oxidative metabolism–related processes during RL after disuse, clustering of human skeletal muscle biochemical and physiologic parameters was performed with the SciPy (v.0.19.1) toolkit (41). The RL response (RL–UL) per parameter was expressed as the percentage change from UL. The Spearman correlation coefficient between each pair of relative RL responses (*i.e.*, $R_{j,k}$) was computed and subsequently transformed to Euclidean distance ($D_{j,k}$) with (Eq. 1):

$$D_{j,k} = \sqrt{1 - |R_{j,k}|} \quad (1)$$

The resulting Euclidean distance matrix was hierarchically clustered based on the between-cluster average linkage using SciPy's *cluster.hierarchy.linkage* module and visualized using the clustermap module within Seaborn v.0.8.1 (42). Differences in the distribution of markers between clusters were tested by Pearson's χ^2 test with *post hoc* analysis based on adjusted residuals with Bonferroni correction.

The RL response per parameter of paired data (human biopsies) was tested by paired-samples *t* test. The time-dependent RL response (mouse muscle) was tested by 1-way ANOVA with Dunnett's *post hoc* test, using UL as a reference group. Data are expressed as means ± SEM, unless indicated otherwise. Statistical analyses were performed with SPSS Statistics (v.22.0; IBM, Armonk, NY, USA).

RESULTS

One week of remobilization after leg immobilization–induced atrophy tended to increase quadriceps CSA (**Table 1**). However, neither quadriceps CSA nor muscle force measured by 1-RM had returned to preimmobilization baseline levels, indicating that recovery was still ongoing.

Regulators and mediators of myogenesis, autophagy, and mitochondrial mass and dynamics correlate during recovery from muscle disuse in humans

To address whether there is a correlation between alterations in skeletal muscle mass– and oxidative metabolism–related processes during RL after disuse, we measured the protein and mRNA expression of several regulators and mediators of protein turnover, mitochondrial turnover, and myonuclear turnover, before and after 7 d of RL in humans and clustered the correlations between relative RL responses based on similarity. From this, 4 clusters of parameters were identified (**Fig. 1**).

Cluster 1 appeared enriched in markers of protein turnover signaling, whereas cluster 2 seemed to be enriched in markers of muscle mass and function (Supplemental Table S3). Furthermore, two major clusters (3, 4) occurred in which markers of myogenesis and autophagy were strongly represented (Supplemental Table S3). This strong representation of myogenesis and autophagy markers was accompanied by a high percentage of markers of mitochondrial turnover and mitochondrial dynamics in cluster 3, whereas cluster 4 was concomitantly enriched in markers of mitochondrial mass and appeared enriched in markers of mitochondrial dynamics, and to some extent, protein turnover (Supplemental Table S3). Furthermore, most of the myogenesis markers represented in cluster 3 [*i.e.*, myogenic factor (*MYF*)-5, myosin heavy chain (*MYH*)-8, myogenin (*MYOG*), and *MYH9* mRNA] are associated with late stages of myogenesis (*i.e.*, differentiation and fusion), whereas most of the myogenesis regulators and markers represented in cluster 4 [*i.e.*, myostatin (MSTN) protein, and cyclin D1, *PAX7*, and cadherin 15 mRNA] are associated with early stages of myogenesis (*i.e.*, proliferation). Moreover, most of the autophagy markers in cluster 3 [*i.e.*, optineurin (*OPTN*) mRNA, and microtubule associated protein 1 light chain 3 β (MAP1LC3B)-II, MAP1LC3B-I, and beclin (BECN)-1 protein] are indicators of autophagosome formation, whereas most of the autophagy markers in cluster 4 [*i.e.*, phosphorylated unc-51–like autophagy-activating kinase 1 (ULK1) ser556, pULK1ser556:ULK1 ratio, pULK1ser758, pULK1ser758:ULK1 ratio, GABA type A receptor–associated protein-like 1 (GABARAPL1), and sequestosome 1 (SQSTM1) protein] are indicators of autophagy initiation.

Induction of late myogenic markers after 5 d of RL in mice

The distinct clustering of early (cluster 4) and late (cluster 3) myogenesis markers upon remobilization in human subjects may reflect a time-dependent expression pattern of these markers, as previously observed for early myogenesis markers by Pansters *et al.* (30). This RL time-course mouse study was therefore used to address those time-dependent expression patterns. In this study, UL decreased the myofiber CSA, myonuclear domain, and number of nuclei per fiber (**Fig. 2*A*–*C***). Ongoing recovery was indicated by an incomplete normalization of CSA and myonuclear domain up to RL-8, and the number of nuclei per fiber was significantly restored at RL-3 and -8. This restoration of the myonuclei was paralleled by a tendency toward an increased number of SCs at RL-3 (Fig. 2*D, E*).

To assess whether late myogenesis markers indeed display a distinct temporal expression pattern, we measured markers of SC fusion and early myofiber regeneration in mouse gastrocnemius at 1, 2, 3, 5, and 8 d of RL after hindlimb suspension. At RL-1 and -2, *Myh9* was transiently increased and gradually normalized at RL-5 and -8 (**Fig. 3**). The expression of another, novel fusion marker, myomaker (*Mymk*), was strongly but transiently induced at RL-5. Furthermore, *Myh8* was induced at RL-5 and -8. Expression of the muscle-specific gene creatine kinase (*Ckm*) was reduced upon UL, and was transiently further reduced at RL-1, -2, and -3, whereas expression of the negative regulator of muscle mass *Mstn* was reduced at RL-5 and -8.

Parallel modulation of autophagy and myogenesis in mice

To address whether the temporal expression patterns of early and late myogenesis markers coincide with a temporal regulation of autophagy (as suggested from clusters

TABLE 1. *Response to immobilization*

Parameter	Preimmobilization	Postimmobilization	Remobilization
Body weight (kg)	70.9 ± 3.3	72.0 ± 3.2	71.7 ± 3.1
Quadriceps CSA (mm^2)	8004 ± 320	7562 ± 303***	7671 ± 315**,#
1-RM (kg)	57 ± 3	50 ± 2**	52 ± 2*

Data are expressed as means ± SEM. *$P < 0.05$, **$P < 0.01$, ***$P < 0.001$ *vs.* preimmobilization, #$P < 0.1$ *vs.* postimmobilization.

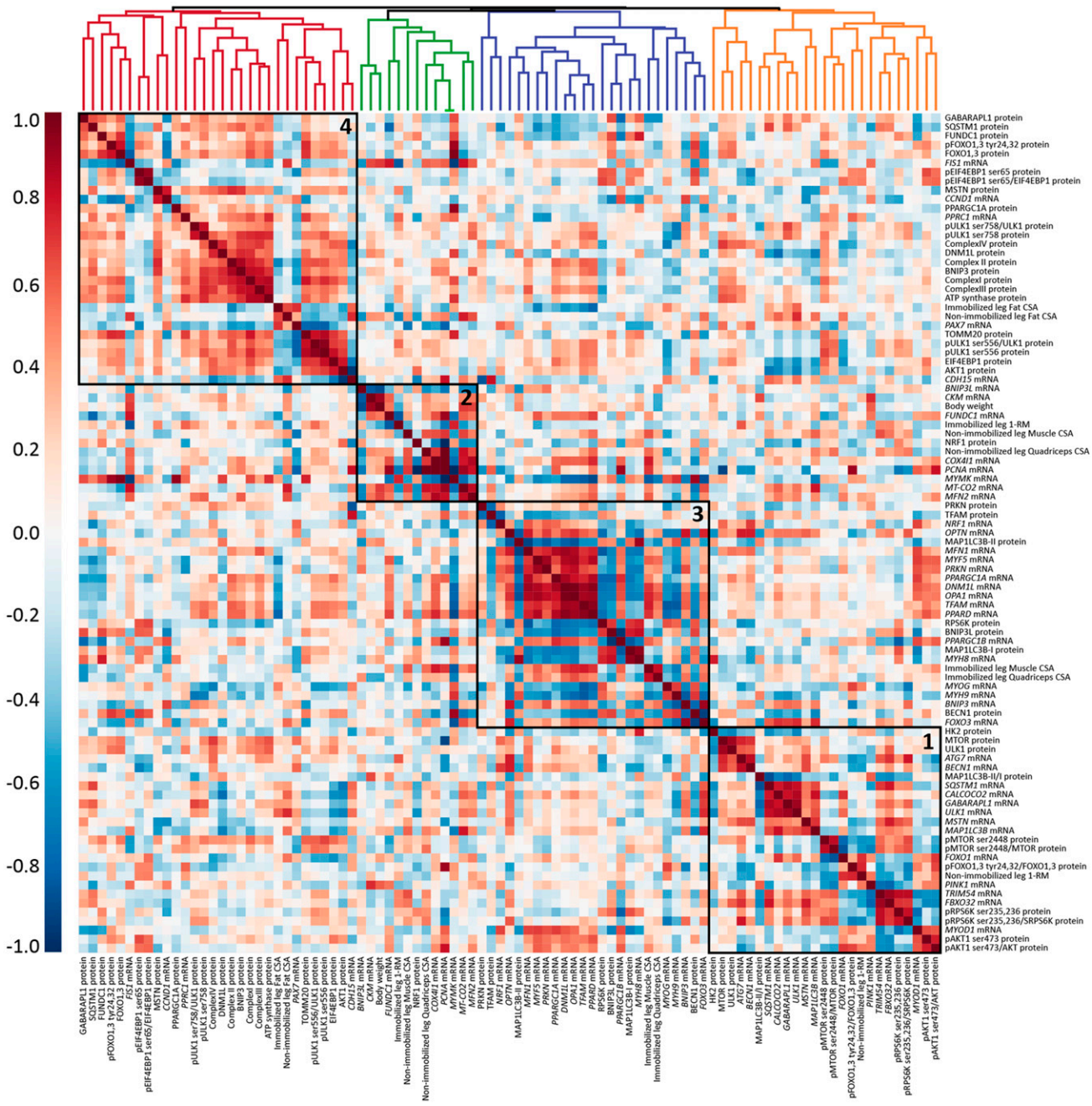

Figure 1. A correlation heatmap and cluster dendrogram of biochemical and functional parameters during skeletal muscle recovery from disuse in humans. Each square represents the Spearman correlation coefficient between the relative RL responses of parameters displayed on the *x*- and *y*-axes, with colors indicating the strength and direction of the correlation.

3 and 4), mRNA and protein levels of indicators of autophagosome formation and markers of autophagy capacity and autophagy initiation were measured.

The relative protein expression of Map1lc3b-I displayed an acute but transient increase at RL-1, -2, and -3, whereas Map1lc3b-II levels remained largely unaltered (**Fig. 4**). The Map1lc3b-II:I ratio was decreased at RL-1, but subsequently normalized, and even increased at RL-8. Furthermore, the relative mRNA expression of *Map1lc3b* was decreased at RL-2, -3, and -5, and seemed to be partially normalized at RL-8 (**Fig. 5**). In contrast, Gabarapl1 and Sqstm1 protein and mRNA expression displayed an acute but transient increase at RL-1 compared to UL, although *Gabarapl1* mRNA was initially reduced upon UL (Figs. 4 and 5). The mRNA expression of *Optn*, *Becn1*, and autophagy related-7 were unaltered during RL (Fig. 5).

To further address a main regulatory step in the conversion of changes in autophagy capacity into flux, the activating and inhibiting phosphorylation of Ulk1 was assessed. Both absolute and relative activating Ulk1 phosphorylation (ser555) were increased during RL, up to RL-3 (**Fig. 6**). However, in parallel, both absolute and relative inhibiting Ulk1 phosphorylation (ser757) were increased during RL, up to RL-5.

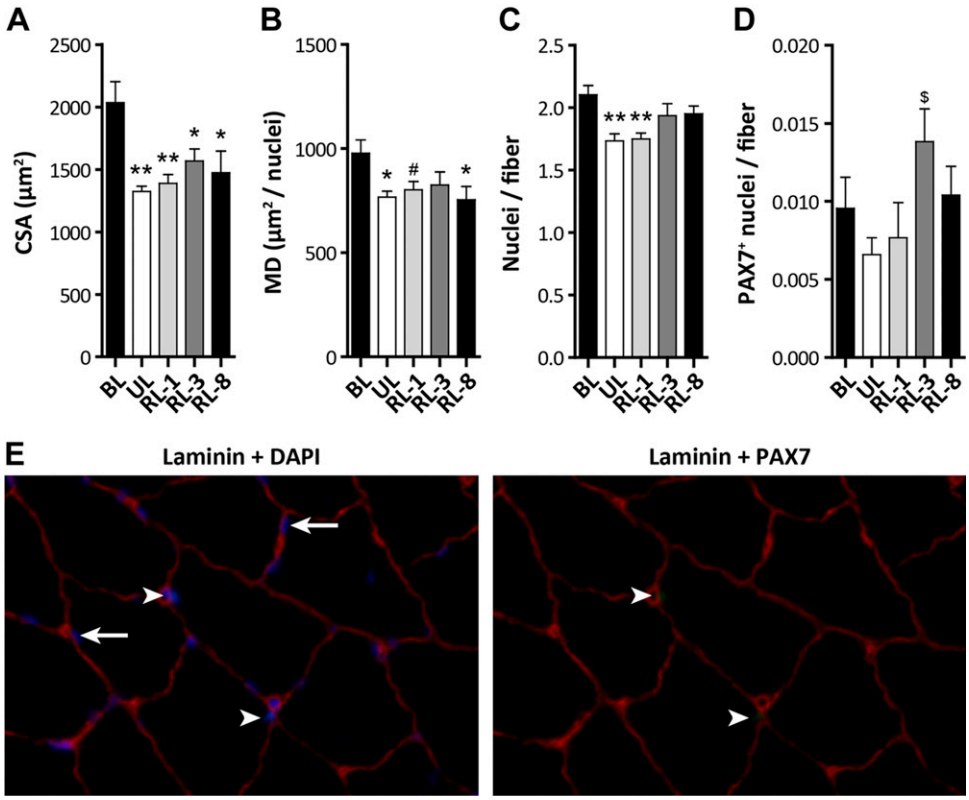

Figure 2. Changes in myofiber CSA, myonuclear domain (MD), and the number of myonuclei and SCs during muscle disuse and recovery in mice. *A–D*) Gastrocnemius muscles were collected at baseline (BL), after 14 d of UL, or after 1, 3, or 8 d of RL, for immunohistochemical determination of mean muscle fiber CSA (*A*); MD (*B*); mean number of myonuclei (*C*); and mean number of PAX7$^+$ SCs per muscle fiber (*D*). *E*) Representation of immunohistochemical detection of laminin (red) and PAX7 (green), and nuclei stained with DAPI (blue). Arrowheads: PAX7$^+$ SCs, arrows: myofiber nuclei. $^{\#}P < 0.1$, $^{*}P < 0.05$, $^{**}P < 0.01$, *vs.* BL, and $^{\$}P < 0.05$ *vs.* UL.

Temporal induction of mitophagy during recovery from disuse in mice

Next to the predominance of markers of autophagosome formation in cluster 3, this cluster also appeared to be enriched in markers of mitophagy. We therefore assessed the temporal expression of mitophagy markers during recovery from disuse in mice.

No significant alterations in protein expression of BCL2 interacting protein 3 like (Bnip3l) or parkin RBR E3 ubiquitin protein ligase (Prkn) were observed during recovery after disuse. However, the protein expression of Bnip3 increased at RL-1, subsequently returned to UL values, and decreased at RL-5 and -8 (**Fig. 7**). Furthermore, FUN14 domain containing 1 (Fundc1) protein expression was increased at RL-8 compared to UL, although an initial decrease was observed upon UL. Corresponding to its change in protein abundance, *Fundc1* mRNA expression was increased at RL-8 (**Fig. 8**). Furthermore, *Bnip3l* mRNA expression was decreased, and phosphatase and tensin homolog (PTEN)-induced putative kinase (*Pink*)-1 tended to be decreased upon remobilization, up to d RL-8, but no changes in the expression of *Prkn* mRNA were observed.

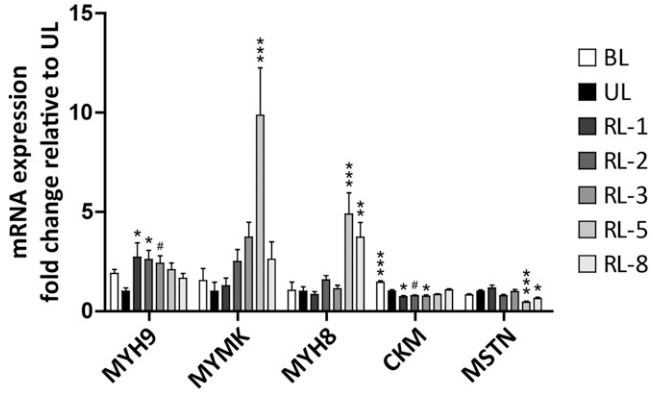

Figure 3. Temporal changes in mRNA expression of markers and mediators of late myogenesis upon recovery from muscle disuse in mice. mRNA expression of MYH9, MYMK, MYH8, creatine kinase, and MSTN was assessed in gastrocnemius upon recovery from 14 d hindlimb suspension. $^{\#}P < 0.1$, $^{*}P < 0.05$, $^{**}P < 0.01$, $^{***}P < 0.001$ *vs.* UL.

DISCUSSION

Alterations in the regulation of both muscle mass and metabolic plasticity during recovery from disuse have been reported, but the interaction between these processes is understudied. Hence, we explored this potential interaction by measuring established molecular regulators and mediators of processes that determine muscle mass and metabolism in human and mouse muscle and showed that molecular markers of myogenesis, autophagy, and mitochondrial mass and dynamics change coordinately during recovery from disuse.

In the current human study, 1 wk of remobilization after leg immobilization-induced atrophy increased quadriceps CSA compared to postimmobilization, but did not return quadriceps CSA or muscle force measured by 1-RM to preimmobilzation baseline levels. This finding is in line with those in studies that showed an incomplete normalization of CSA (43, 44) and muscle strength (44) upon 1 wk of recovery after immobilization and a complete

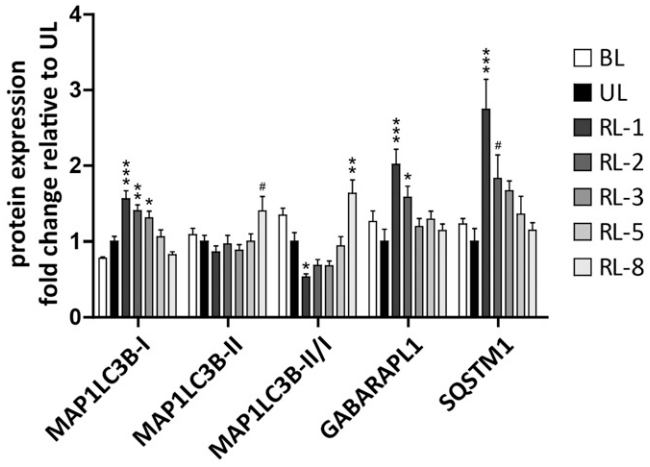

Figure 4. Temporal changes in protein expression of autophagosome formation indicators upon recovery from muscle disuse in mice. Protein expression of MAP1LC3B-I, MAP1LC3B-II, MAP1LC3B-II:I, GABARAPL1, and SQSTM1 was assessed in gastrocnemius upon recovery from 14 d hindlimb suspension. $^{\#}P < 0.1$, $^{*}P < 0.05$, $^{**}P < 0.01$, $^{***}P < 0.001$ *vs.* UL.

normalization of muscle mass and strength after 2 wk of recovery (25, 44–47). This result shows that after 1 wk of remobilization, skeletal muscle recovery is still ongoing, and thus allows us to study the processes that are associated with recovery.

We detected substantial interindividual variation in the human molecular responses to RL (Supplemental Fig. S1), which was not affected by correction for creatine supplementation. We exploited this variation to assess the relation between molecular RL responses. Based on hierarchical cluster analysis of the correlations between relative RL responses, we identified 4 clusters of parameters. The coappearance of markers and mediators of classic muscle mass– and oxidative metabolism–related processes within clusters 3 and 4 may point at an interdependency or joint regulation of these processes during recovery from atrophy. Although we cannot exclude creatine supplementation as a potential confounding factor and a modulatory effect of creatine supplementation on certain molecular processes has been suggested (48, 49), there is no indication of an effect of creatine supplementation on the interrelationship between the regulatory processes associated with recovery from muscle atrophy, and correction for creatine supplementation does not alter the pattern of correlations between RL effects. Markers that regulate and mediate different stages of myogenesis and autophagy displayed a distinct clustering, which may be related to differences in their temporal expression patterns. Between-subject asynchronicity in such temporal expression patterns may contribute to the observed variation, which—despite its applicability in the assessment of between-variable associations—limits the statistical power to detect relevant changes on a group level. Furthermore, interindividual asynchronicity, combined with a single time-point observation during recovery in humans, complicates the synthesis of a univocal conclusion on the molecular RL response. The high-resolution time-course study in mice was thus instrumental in the in-depth exploration of the time-dependent molecular regulation of muscle mass and metabolic plasticity during disuse-induced atrophy recovery.

Similar to the study in humans, mice displayed an incomplete normalization of muscle weight (30) and muscle fiber CSA, which supports ongoing recovery over 8 d of RL. Three days of RL after hindlimb suspension transiently increased the number of $PAX7^{+}$ SCs per fiber. This finding is in line with previous studies assessing SC numbers after relative short-term remobilization in rodents (50–52) and humans (46) and may explain the unaltered number of SCs upon longer term remobilization (53). In accordance with the early induction of SC proliferation, our lab showed in another study an early and potentially biphasic induction of markers and mediators of the initial steps in myogenesis in this model (30). In the current work, we showed for the first time that, subsequent to this increase in early myogenesis markers, the markers and mediators of late stages of myogenesis *Mymk* and *Myh8* are increased toward the end of the 8 d RL phase. Furthermore, in line with refs. 54 and 56, there was a partial restoration of the number of nuclei per fiber after 3 d of RL, which supports the notion that SCs functionally contribute to skeletal muscle recovery after disuse (57). Indeed, because the myonuclear domain was unaltered during remobilization, the increase in myonuclear content is expected to result in an increase in muscle fiber CSA. However, as this change in fiber CSA is not yet significantly detectable, we conclude that muscle fiber CSA is incompletely restored up to 8 d of remobilization. These findings could be speculated to result from a lag time between myonuclear accretion and a functional contribution of the newly incorporated nucleus to protein synthesis or to reflect a role for myonuclear accretion in muscle fiber metabolic plasticity. Despite the incomplete normalization of muscle fiber CSA and myonuclear domain over the time course examined in this mouse study, their recovery seemed to start as early as RL-1. This is in agreement with

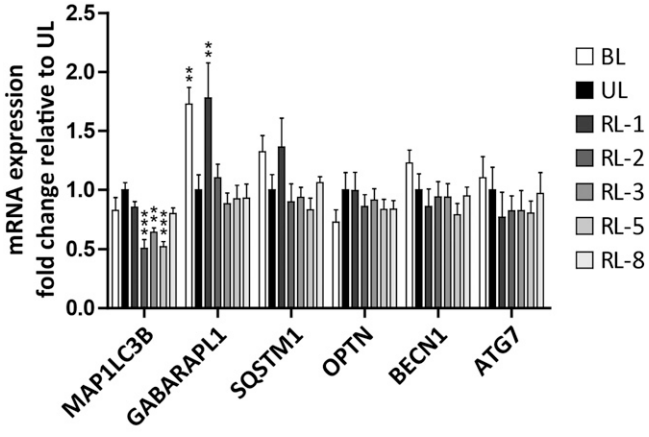

Figure 5. Temporal changes in mRNA expression of autophagy-related genes upon recovery from muscle disuse in mice. mRNA expression of MAP1LC3B, GABARAPL1, SQSTM1, OPTN, BECN1, and autophagy related (ATG)-7 was assessed in gastrocnemius upon recovery from 14 d hindlimb suspension. $^{**}P < 0.01$, $^{***}P < 0.001$ *vs.* UL.

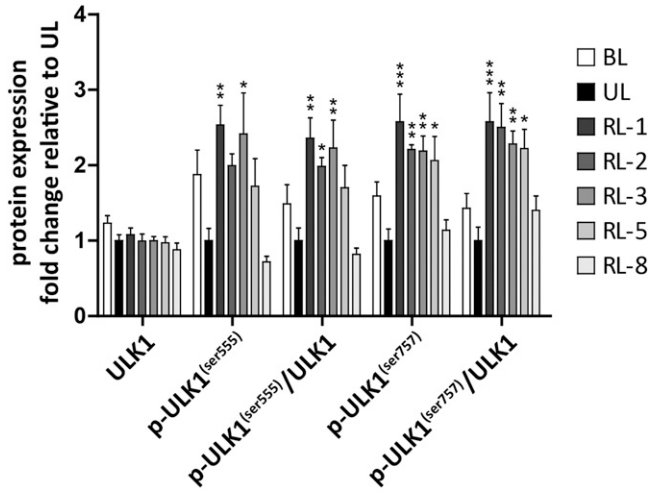

Figure 6. Temporal changes in protein expression of markers of autophagy initiation upon recovery from muscle disuse in mice. Protein expression of ULK1, p-ULK1(ser555), p-ULK1(ser555):ULK1 ratio, p-ULK1(ser757), and p-ULK1(ser757):ULK1 ratio was assessed in gastrocnemius upon recovery from 14 d hindlimb suspension. $^{*}P < 0.05$, $^{**}P < 0.01$, $^{***}P < 0.001$ *vs.* UL.

the previously observed acute and sustained increase in protein synthesis signaling (30, 58–60) and increased protein synthesis rates upon RL (61). This anabolic state precedes myonuclear accretion, which supports the notion that hypertrophy can occur to some extent independent of SCs (62). Furthermore, previous studies have consistently shown a suppression of mediators of the UPS during recovery from disuse (27, 30, 44, 52, 59, 60, 63–65), whereas a transient increase in proteasome activity (27, 61) and ubiquitin-conjugated proteins (60) have been observed simultaneously.

In this study, we conducted a comprehensive analysis of markers of autophagosome formation, autophagy capacity, and autophagy initiation. From this, we conclude that autophagy is actively regulated both acutely, as well as after 5 and 8 d of RL, which appears to parallel the temporal regulation of myonuclear accretion. We showed an acute but transient increase in the autophagosome formation markers Map1lc3b-I, Gabarapl1, and Sqstm1 protein, and a decrease and subsequent increase in the Map1lc3b-II:I ratio that parallels the regulation of late stages of myogenesis. In line with our data, previous studies showed an increase in Sqstm1 protein expression (27) and an increase in Map1lc3b-II:I ratio (31). In addition, White *et al.* (63) reported an unaltered Map1lc3b-II:I ratio after 14 d of RL, potentially reflecting a normalization of autophagy signaling upon completed recovery. Furthermore, in line with previous studies (59, 66), we showed a transient decrease in the mRNA expression of the autophagy capacity indicator *Map1lc3b* and a transient increase in the mRNA expression of *Gabarapl1* relative to UL. In addition to the reported increase in Ulk1 inhibiting phosphorylation (27, 29), we report a concomitant induction of Ulk1 inhibiting and activating phosphorylation. This temporal regulation of autophagy initiation resembles the expression pattern of early myogenesis markers observed by Pansters *et al.* (30).

Despite our comprehensive analysis of autophagy regulation, we did not measure autophagy flux and therefore cannot draw an unambiguous conclusion regarding the net effect of RL on the autophagy flux itself. Furthermore, alterations in expression levels of several autophagy regulators and mediators seem contradictory, which emphasizes the complexity of autophagy regulation during recovery after disuse. We speculate that this complexity reflects the degradation of specific targets (*e.g.*, mitochondria), which is in accordance with a possible involvement of autophagy in skeletal muscle metabolic plasticity in addition to its classic role in muscle mass regulation (67, 68). Recent papers suggest a crucial role for autophagy, and more specifically, mitophagy, in skeletal muscle functional regeneration (69, 70).

During recovery after disuse in mice, the gene expression of the mitochondrial damage-related mitophagy regulator *Pink1* tends to be decreased, whereas *Prkn* is unaltered. In addition, Prkn protein expression is unaltered during remobilization, although it should be noted that this mitophagy pathway is also modulated by post-translational modifications (71), which were not assessed in this study. Receptor-mediated mitophagy *via* BNIP3L, BNIP3, and FUNDC1 can be induced by both hypoxia and increased oxidative stress (72), of which an increase during RL has been documented (73, 74). Bnip3 protein expression transiently increased, and subsequently decreased during recovery, which parallels the previously reported alterations in *Bnip3* mRNA expression in this mouse study (30), and the increase in Bnip3 protein expression reported by Kang and Ji (74). In contrast, Bnip3l protein expression is unaltered upon recovery after disuse, whereas *Bnip3l* mRNA expression displays a persistent decrease up to RL-5. The mRNA and protein expression of Fundc1 is specifically induced at RL-8, suggesting a late-phase response.

These molecular alterations point toward a temporal induction of mitophagy both acutely and after 8 d of recovery after disuse. Nevertheless, previous data suggest a normalization of mitochondrial content upon several days of RL (34, 73–75), likely driven by an increase in

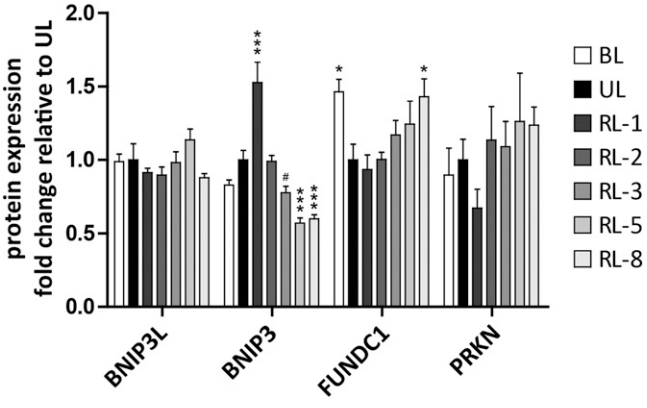

Figure 7. Temporal changes in protein expression of mitophagy regulators and mediators upon recovery from muscle disuse in mice. Protein expression of BNIP3L, BNIP3, FUNDC1, and PRKN was assessed in gastrocnemius upon recovery from 14 d hindlimb suspension. $^{\#}P < 0.1$, $^{*}P < 0.05$, $^{***}P < 0.001$ *vs.* UL.

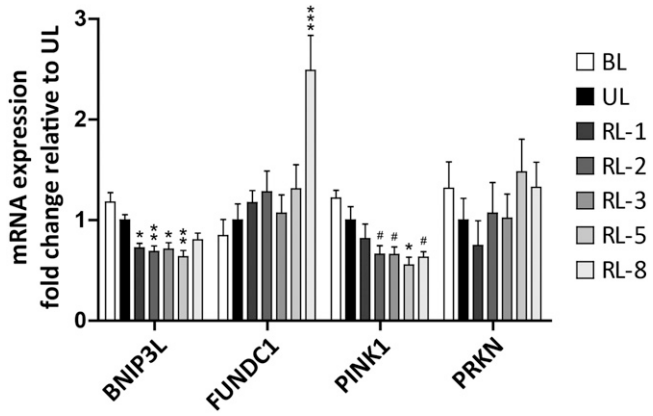

Figure 8. Temporal changes in mRNA expression of mitophagy-related genes upon recovery from muscle disuse in mice. mRNA expression of BNIP3L, BNIP3, FUNDC1, PINK1, and PRKN was assessed in gastrocnemius upon recovery from 14 d hindlimb suspension. $^{\#}P < 0.1$, $^{*}P < 0.05$, $^{**}P < 0.01$, $^{***}P < 0.001$ *vs.* UL.

mitochondrial biogenesis (34, 73). The induction of mitophagy in the presence of a recovery of mitochondrial content suggests the induction of mitochondrial remodeling during remobilization. Indeed, an increase in mitochondrial remodeling (75) and mitochondrial dynamics (34, 75) has been observed during recovery from disuse. This RL-induced mitochondrial remodeling may be a response to increased oxphos (76) and could serve to meet the altered metabolic demands during remobilization. Another observation is that a late increase in Fundc1 expression paralleled the temporal regulation of late-stage myogenesis markers. It is becoming increasingly clear that mitophagy (77), mitochondrial dynamics (78, 79), and metabolic reprogramming (80–83) are crucial for myogenic differentiation. Furthermore, Mishra *et al.* (76) showed that mitochondrial proteins compartmentalize to discrete domains located around a nucleus of origin that originates from SC-mediated myonuclear accretion. In line, myogenesis seems to be involved in the aerobic adaptation in response to endurance-type exercise (84). Clearly, this indicates a close relation between muscle mass– and oxidative metabolism–related processes.

CONCLUSIONS

We showed, through the combination of a cluster analysis and high-resolution time-course study, that the molecular regulation of protein turnover, mitochondrial turnover, and myonuclear turnover are correlated and temporally associated during recovery from atrophy. This result suggests an interdependency or joint regulation of these muscle mass– and oxidative metabolism–related processes during recovery from atrophy and emphasizes the need to study these processes by integrated molecular analyses. FJ

ACKNOWLEDGMENTS

The authors thank Marco Kelders, Chiel de Theije, and Antoine Zorenc (all of Maastricht University) for excellent technical assistance in performing the molecular analyses, and Roy Haast (Maastricht Centre for Systems Biology, Maastricht University) for support in conducting the cluster analysis. The original work from which human muscle biopsies were obtained (36) was funded by TI Food and Nutrition, a public–private partnership for precompetitive research in food and nutrition; and the mouse study was funded by Grant NAF 3.2.07.017 from the Lung Foundation/Netherlands Asthma Foundation and the transnational University Limburg (tUL). For the current work, the researchers had sole responsibility for the study design, data collection and analysis, decision to publish, and preparation of the manuscript. The authors declare no conflicts of interest.

AUTHOR CONTRIBUTIONS

A. Kneppers, P. Leermakers, H. Gosker, L. van Loon, A. Schols, R. Langen, and L. Verdijk designed the research; A. Kneppers, P. Leermakers, E. Backx, and N. Pansters performed the research; A. Kneppers analyzed the data; A. Kneppers, P. Leermakers, R. Langen, and L. Verdijk wrote the manuscript; and all authors read and approved the final manuscript.

REFERENCES

1. Egan, B., and Zierath, J. R. (2013) Exercise metabolism and the molecular regulation of skeletal muscle adaptation. *Cell Metab.* **17**, 162–184
2. Wall, B. T., and van Loon, L. J. (2013) Nutritional strategies to attenuate muscle disuse atrophy. *Nutr. Rev.* **71**, 195–208
3. Wall, B. T., Dirks, M. L., Snijders, T., Senden, J. M., Dolmans, J., and van Loon, L. J. (2014) Substantial skeletal muscle loss occurs during only 5 days of disuse. *Acta Physiol. (Oxf.)* **210**, 600–611
4. Brooks, N. E., and Myburgh, K. H. (2014) Skeletal muscle wasting with disuse atrophy is multi-dimensional: the response and interaction of myonuclei, satellite cells and signaling pathways. *Front. Physiol.* **5**, 99
5. Bierbrauer, J., Koch, S., Olbricht, C., Hamati, J., Lodka, D., Schneider, J., Luther-Schröder, A., Kleber, C., Faust, K., Wiesener, S., Spies, C. D., Spranger, J., Spuler, S., Fielitz, J., and Weber-Carstens, S. (2012) Early type II fiber atrophy in intensive care unit patients with nonexcitable muscle membrane. *Crit. Care Med.* **40**, 647–650
6. Pette, D., and Staron, R. S. (2001) Transitions of muscle fiber phenotypic profiles. *Histochem. Cell Biol.* **115**, 359–372
7. Yu, Z. B., Gao, F., Feng, H. Z., and Jin, J. P. (2007) Differential regulation of myofilament protein isoforms underlying the contractility changes in skeletal muscle unloading. *Am. J. Physiol. Cell Physiol.* **292**, C1192–C1203
8. Stein, T. P., and Wade, C. E. (2005) Metabolic consequences of muscle disuse atrophy. *J. Nutr.* **135**, 1824S–1828S
9. Gram, M., Dahl, R., and Dela, F. (2014) Physical inactivity and muscle oxidative capacity in humans. *Eur. J. Sport Sci.* **14**, 376–383
10. Dirks, M. L., Wall, B. T., van de Valk, B., Holloway, T. M., Holloway, G. P., Chabowski, A., Goossens, G. H., and van Loon, L. J. (2016) One week of bed rest leads to substantial muscle atrophy and induces whole-body insulin resistance in the absence of skeletal muscle lipid accumulation. *Diabetes* **65**, 2862–2875
11. Gram, M., Vigelsø, A., Yokota, T., Helge, J. W., Dela, F., and Hey-Mogensen, M. (2015) Skeletal muscle mitochondrial H_2O_2 emission increases with immobilization and decreases after aerobic training in young and older men. *J. Physiol.* **593**, 4011–4027
12. Romanello, V., Guadagnin, E., Gomes, L., Roder, I., Sandri, C., Petersen, Y., Milan, G., Masiero, E., Del Piccolo, P., Foretz, M., Scorrano, L., Rudolf, R., and Sandri, M. (2010) Mitochondrial fission and remodelling contributes to muscle atrophy. *EMBO J.* **29**, 1774–1785
13. Seene, T., Kaasik, P., and Riso, E. M. (2012) Review on aging, unloading and reloading: changes in skeletal muscle quantity and quality. *Arch. Gerontol. Geriatr.* **54**, 374–380
14. Rizzoli, R., Reginster, J. Y., Arnal, J. F., Bautmans, I., Beaudart, C., Bischoff-Ferrari, H., Biver, E., Boonen, S., Brandi, M. L., Chines, A.,

Cooper, C., Epstein, S., Fielding, R. A., Goodpaster, B., Kanis, J. A., Kaufman, J. M., Laslop, A., Malafarina, V., Mañas, L. R., Mitlak, B. H., Oreffo, R. O., Petermans, J., Reid, K., Rolland, Y., Sayer, A. A., Tsouderos, Y., Visser, M., and Bruyère, O. (2013) Quality of life in sarcopenia and frailty. *Calcif. Tissue Int.* **93**, 101–120
15. Schols, A. M., Broekhuizen, R., Weling-Scheepers, C. A., and Wouters, E. F. (2005) Body composition and mortality in chronic obstructive pulmonary disease. *Am. J. Clin. Nutr.* **82**, 53–59
16. Martin, L., Birdsell, L., Macdonald, N., Reiman, T., Clandinin, M. T., McCargar, L. J., Murphy, R., Ghosh, S., Sawyer, M. B., and Baracos, V. E. (2013) Cancer cachexia in the age of obesity: skeletal muscle depletion is a powerful prognostic factor, independent of body mass index. *J. Clin. Oncol.* **31**, 1539–1547
17. Marzetti, E., Calvani, R., Tosato, M., Cesari, M., Di Bari, M., Cherubini, A., Collamati, A., D'Angelo, E., Pahor, M., Bernabei, R., Landi, F., and Consortium, S.; SPRINTT Consortium. (2017) Sarcopenia: an overview. *Aging Clin. Exp. Res.* **29**, 11–17
18. Dirks, M. L., Wall, B. T., Snijders, T., Ottenbros, C. L., Verdijk, L. B., and van Loon, L. J. (2014) Neuromuscular electrical stimulation prevents muscle disuse atrophy during leg immobilization in humans. *Acta Physiol. (Oxf.)* **210**, 628–641
19. Dirks, M. L., Wall, B. T., Nilwik, R., Weerts, D. H., Verdijk, L. B., and van Loon, L. J. (2014) Skeletal muscle disuse atrophy is not attenuated by dietary protein supplementation in healthy older men. *J. Nutr.* **144**, 1196–1203
20. Ferrando, A. A., Paddon-Jones, D., Hays, N. P., Kortebein, P., Ronsen, O., Williams, R. H., McComb, A., Symons, T. B., Wolfe, R. R., and Evans, W. (2010) EAA supplementation to increase nitrogen intake improves muscle function during bed rest in the elderly. *Clin. Nutr.* **29**, 18–23
21. Paddon-Jones, D., Sheffield-Moore, M., Urban, R. J., Sanford, A. P., Aarsland, A., Wolfe, R. R., and Ferrando, A. A. (2004) Essential amino acid and carbohydrate supplementation ameliorates muscle protein loss in humans during 28 days bedrest. *J. Clin. Endocrinol. Metab.* **89**, 4351–4358
22. Reidy, P. T., McKenzie, A. I., Brunker, P., Nelson, D. S., Barrows, K. M., Supiano, M., LaStayo, P. C., and Drummond, M. J. (2017) Neuromuscular electrical stimulation combined with protein ingestion preserves thigh muscle mass but not muscle function in healthy older adults during 5 days of bed rest. *Rejuvenation Res.* **20**, 449–461
23. Dideriksen, K., Boesen, A. P., Kristiansen, J. F., Magnusson, S. P., Schjerling, P., Holm, L., and Kjaer, M. (2016) Skeletal muscle adaptation to immobilization and subsequent retraining in elderly men: no effect of anti-inflammatory medication. *Exp. Gerontol.* **82**, 8–18
24. Tanner, R. E., Brunker, L. B., Agergaard, J., Barrows, K. M., Briggs, R. A., Kwon, O. S., Young, L. M., Hopkins, P. N., Volpi, E., Marcus, R. L., LaStayo, P. C., and Drummond, M. J. (2015) Age-related differences in lean mass, protein synthesis and skeletal muscle markers of proteolysis after bed rest and exercise rehabilitation. *J. Physiol.* **593**, 4259–4273
25. Suetta, C., Hvid, L. G., Justesen, L., Christensen, U., Neergaard, K., Simonsen, L., Ortenblad, N., Magnusson, S. P., Kjaer, M., and Aagaard, P. (2009) Effects of aging on human skeletal muscle after immobilization and retraining. *J. Appl. Physiol.* **107**, 1172–1180
26. Joanisse, S., Nederveen, J. P., Snijders, T., McKay, B. R., and Parise, G. (2017) Skeletal muscle regeneration, repair and remodelling in aging: the importance of muscle stem cells and vascularization. *Gerontology* **63**, 91–100
27. Baehr, L. M., West, D. W., Marcotte, G., Marshall, A. G., De Sousa, L. G., Baar, K., and Bodine, S. C. (2016) Age-related deficits in skeletal muscle recovery following disuse are associated with neuromuscular junction instability and ER stress, not impaired protein synthesis. *Aging (Albany N.Y.)* **8**, 127–146
28. Thériault, M. E., Paré, M. E., Lemire, B. B., Maltais, F., and Debigaré, R. (2014) Regenerative defect in vastus lateralis muscle of patients with chronic obstructive pulmonary disease. *Respir. Res.* **15**, 35
29. Kelleher, A. R., Pereira, S. L., Jefferson, L. S., and Kimball, S. R. (2015) REDD2 expression in rat skeletal muscle correlates with nutrient-induced activation of mTORC1: responses to aging, immobilization, and remobilization. *Am. J. Physiol. Endocrinol. Metab.* **308**, E122–E129
30. Pansters, N. A., Schols, A. M., Verhees, K. J., de Theije, C. C., Snepvangers, F. J., Kelders, M. C., Ubags, N. D., Haegens, A., and Langen, R. C. (2015) Muscle-specific GSK-3β ablation accelerates regeneration of disuse-atrophied skeletal muscle. *Biochim. Biophys. Acta* **1852**, 490–506
31. Takahashi, H., Suzuki, Y., Mohamed, J. S., Gotoh, T., Pereira, S. L., and Alway, S. E. (2017) Epigallocatechin-3-gallate increases autophagy signaling in resting and unloaded plantaris muscles but selectively suppresses autophagy protein abundance in reloaded muscles of aged rats. *Exp. Gerontol.* **92**, 56–66
32. Kang, C., Yeo, D., and Ji, L. L. (2016) Muscle immobilization activates mitophagy and disrupts mitochondrial dynamics in mice. *Acta Physiol. (Oxf.)* **218**, 188–197
33. McClung, J. M., Davis, J. M., Wilson, M. A., Goldsmith, E. C., and Carson, J. A. (2006) Estrogen status and skeletal muscle recovery from disuse atrophy. *J. Appl. Physiol.* **100**, 2012–2023
34. Remels, A. H., Pansters, N. A., Gosker, H. R., Schols, A. M., and Langen, R. C. (2014) Activation of alternative NF-κB signaling during recovery of disuse-induced loss of muscle oxidative phenotype. *Am. J. Physiol. Endocrinol. Metab.* **306**, E615–E626
35. López-Lluch, G. (2017) Essential role of mitochondrial dynamics in muscle physiology. *Acta Physiol. (Oxf.)* **219**, 20–21
36. Backx, E. M. P., Hangelbroek, R., Snijders, T., Verscheijden, M. L., Verdijk, L. B., de Groot, L. C. P. G. M., and van Loon, L. J. C. (2017) Creatine loading does not preserve muscle mass or strength during leg immobilization in healthy, young males: a randomized controlled trial. *Sports Med.* **47**, 1661–1671
37. Bodine, S. C., Latres, E., Baumhueter, S., Lai, V. K., Nunez, L., Clarke, B. A., Poueymirou, W. T., Panaro, F. J., Na, E., Dharmarajan, K., Pan, Z. Q., Valenzuela, D. M., DeChiara, T. M., Stitt, T. N., Yancopoulos, G. D., and Glass, D. J. (2001) Identification of ubiquitin ligases required for skeletal muscle atrophy. *Science* **294**, 1704–1708
38. Ferreira, R., Neuparth, M. J., Ascensão, A., Magalhães, J., Vitorino, R., Duarte, J. A., and Amado, F. (2006) Skeletal muscle atrophy increases cell proliferation in mice gastrocnemius during the first week of hindlimb suspension. *Eur. J. Appl. Physiol.* **97**, 340–346
39. Hanson, A. M., Harrison, B. C., Young, M. H., Stodieck, L. S., and Ferguson, V. L. (2013) Longitudinal characterization of functional, morphologic, and biochemical adaptations in mouse skeletal muscle with hindlimb suspension. *Muscle Nerve* **48**, 393–402
40. Ruijter, J. M., Thygesen, H. H., Schoneveld, O. J., Das, A. T., Berkhout, B., and Lamers, W. H. (2006) Factor correction as a tool to eliminate between-session variation in replicate experiments: application to molecular biology and retrovirology. *Retrovirology* **3**, 2
41. Oliphant, T. E. (2007) Python for scientific computing. *Comput. Sci. Eng.* **9**, 10–20
42. Waskom, M., Botvinnik, O., O'Kane, D., Hobson, P., Lukauskas, S., Gemperline, D. C., Augspurger, T., Halchenko, Y., Cole, J. B., Warmenhoven, J., Ruiter, J. d., Pye, C., Hoyer, S., Verplas, J., Villalba, S., Kunter, G., Quintero, E., Bachant, P., Martin, M., Meyer, K., Miles, A., Ram, Y., Yarkoni, T., Williams, M. L., Evans, C., Fitzgerald, C., Brian, Fonnesbeck, C., Lee, A., Qalieh, A. (2017) mwaskom/seaborn: v.0.8.1 (September 2017). Zenodo, Geneva, Switzerland. Available at: https://doi.org/10.5281/zenodo.883859
43. Hvid, L. G., Suetta, C., Nielsen, J. H., Jensen, M. M., Frandsen, U., Ørtenblad, N., Kjaer, M., and Aagaard, P. (2014) Aging impairs the recovery in mechanical muscle function following 4 days of disuse. *Exp. Gerontol.* **52**, 1–8
44. Jones, S. W., Hill, R. J., Krasney, P. A., O'Conner, B., Peirce, N., and Greenhaff, P. L. (2004) Disuse atrophy and exercise rehabilitation in humans profoundly affects the expression of genes associated with the regulation of skeletal muscle mass. *FASEB J.* **18**, 1025–1027
45. Hortobágyi, T., Dempsey, L., Fraser, D., Zheng, D., Hamilton, G., Lambert, J., and Dohm, L. (2000) Changes in muscle strength, muscle fibre size and myofibrillar gene expression after immobilization and retraining in humans. *J. Physiol.* **524**, 293–304
46. Suetta, C., Frandsen, U., Mackey, A. L., Jensen, L., Hvid, L. G., Bayer, M. L., Petersson, S. J., Schrøder, H. D., Andersen, J. L., Aagaard, P., Schjerling, P., and Kjaer, M. (2013) Ageing is associated with diminished muscle re-growth and myogenic precursor cell expansion early after immobility-induced atrophy in human skeletal muscle. *J. Physiol.* **591**, 3789–3804
47. Hespel, P., Op't Eijnde, B., Van Leemputte, M., Ursø, B., Greenhaff, P. L., Labarque, V., Dymarkowski, S., Van Hecke, P., and Richter, E. A. (2001) Oral creatine supplementation facilitates the rehabilitation of disuse atrophy and alters the expression of muscle myogenic factors in humans. *J. Physiol.* **536**, 625–633
48. Kim, J., Lee, J., Kim, S., Yoon, D., Kim, J., and Sung, D. J. (2015) Role of creatine supplementation in exercise-induced muscle damage: a mini review. *J. Exerc. Rehabil.* **11**, 244–250
49. Deldicque, L., Atherton, P., Patel, R., Theisen, D., Nielens, H., Rennie, M. J., and Francaux, M. (2008) Effects of resistance exercise with and without creatine supplementation on gene expression and cell signaling in human skeletal muscle. *J. Appl. Physiol.* **104**, 371–378

50. Stevens-Lapsley, J. E., Ye, F., Liu, M., Borst, S. E., Conover, C., Yarasheski, K. E., Walter, G. A., Sweeney, H. L., and Vandenborne, K. (2010) Impact of viral-mediated IGF-I gene transfer on skeletal muscle following cast immobilization. *Am. J. Physiol. Endocrinol. Metab.* **299**, E730–E740
51. Ye, F., Mathur, S., Liu, M., Borst, S. E., Walter, G. A., Sweeney, H. L., and Vandenborne, K. (2013) Overexpression of insulin-like growth factor-1 attenuates skeletal muscle damage and accelerates muscle regeneration and functional recovery after disuse. *Exp. Physiol.* **98**, 1038–1052
52. Park, S., Brisson, B. K., Liu, M., Spinazzola, J. M., and Barton, E. R. (2014) Mature IGF-I excels in promoting functional muscle recovery from disuse atrophy compared with pro-IGF-IA. *J. Appl. Physiol.* **116**, 797–806
53. Jackson, J. R., Mula, J., Kirby, T. J., Fry, C. S., Lee, J. D., Ubele, M. F., Campbell, K. S., McCarthy, J. J., Peterson, C. A., and Dupont-Versteegden, E. E. (2012) Satellite cell depletion does not inhibit adult skeletal muscle regrowth following unloading-induced atrophy. *Am. J. Physiol. Cell Physiol.* **303**, C854–C861
54. Mozdziak, P. E., Pulvermacher, P. M., and Schultz, E. (2001) Muscle regeneration during hindlimb unloading results in a reduction in muscle size after reloading. *J. Appl. Physiol.* **91**, 183–190
55. Wang, X. D., Kawano, F., Matsuoka, Y., Fukunaga, K., Terada, M., Sudoh, M., Ishihara, A., and Ohira, Y. (2006) Mechanical load-dependent regulation of satellite cell and fiber size in rat soleus muscle. *Am. J. Physiol. Cell Physiol.* **290**, C981–C989
56. Mitchell, P. O., and Pavlath, G. K. (2004) Skeletal muscle atrophy leads to loss and dysfunction of muscle precursor cells. *Am. J. Physiol. Cell Physiol.* **287**, C1753–C1762
57. Mitchell, P. O., and Pavlath, G. K. (2001) A muscle precursor cell-dependent pathway contributes to muscle growth after atrophy. *Am. J. Physiol. Cell Physiol.* **281**, C1706–C1715
58. Washington, T. A., White, J. P., Davis, J. M., Wilson, L. B., Lowe, L. L., Sato, S., and Carson, J. A. (2011) Skeletal muscle mass recovery from atrophy in IL-6 knockout mice. *Acta Physiol. (Oxf.)* **202**, 657–669
59. Smith, H. K., Matthews, K. G., Oldham, J. M., Jeanplong, F., Falconer, S. J., Bass, J. J., Senna-Salerno, M., Bracegirdle, J. W., and McMahon, C. D. (2014) Translational signalling, atrogenic and myogenic gene expression during unloading and reloading of skeletal muscle in myostatin-deficient mice. *PLoS One* **9**, e94356
60. Kramerova, I., Kudryashova, E., Venkatraman, G., and Spencer, M. J. (2005) Calpain 3 participates in sarcomere remodeling by acting upstream of the ubiquitin-proteasome pathway. *Hum. Mol. Genet.* **14**, 2125–2134
61. Lang, S. M., Kazi, A. A., Hong-Brown, L., and Lang, C. H. (2012) Delayed recovery of skeletal muscle mass following hindlimb immobilization in mTOR heterozygous mice. *PLoS One* **7**, e38910
62. McCarthy, J. J., Mula, J., Miyazaki, M., Erfani, R., Garrison, K., Farooqui, A. B., Srikuea, R., Lawson, B. A., Grimes, B., Keller, C., Van Zant, G., Campbell, K. S., Esser, K. A., Dupont-Versteegden, E. E., and Peterson, C. A. (2011) Effective fiber hypertrophy in satellite cell-depleted skeletal muscle. *Development* **138**, 3657–3666
63. White, J. R., Confides, A. L., Moore-Reed, S., Hoch, J. M., and Dupont-Versteegden, E. E. (2015) Regrowth after skeletal muscle atrophy is impaired in aged rats, despite similar responses in signaling pathways. *Exp. Gerontol.* **64**, 17–32
64. Andrianjafiniony, T., Dupré-Aucouturier, S., Letexier, D., Couchoux, H., and Desplanches, D. (2010) Oxidative stress, apoptosis, and proteolysis in skeletal muscle repair after unloading. *Am. J. Physiol. Cell Physiol.* **299**, C307–C315
65. Chacon-Cabrera, A., Lund-Palau, H., Gea, J., and Barreiro, E. (2016) Time-course of muscle mass loss, damage, and proteolysis in gastrocnemius following unloading and reloading: implications in chronic diseases. *PLoS One* **11**, e0164951
66. Slimani, L., Micol, D., Amat, J., Delcros, G., Meunier, B., Taillandier, D., Polge, C., Béchet, D., Dardevet, D., Picard, B., Attaix, D., Listrat, A., and Combaret, L. (2012) The worsening of tibialis anterior muscle atrophy during recovery post-immobilization correlates with enhanced connective tissue area, proteolysis, and apoptosis. *Am. J. Physiol. Endocrinol. Metab.* **303**, E1335–E1347
67. Ferraro, E., Giammarioli, A. M., Chiandotto, S., Spoletini, I., and Rosano, G. (2014) Exercise-induced skeletal muscle remodeling and metabolic adaptation: redox signaling and role of autophagy. *Antioxid. Redox Signal.* **21**, 154–176
68. Kaur, J., and Debnath, J. (2015) Autophagy at the crossroads of catabolism and anabolism. *Nat. Rev. Mol. Cell Biol.* **16**, 461–472
69. Call, J. A., Wilson, R. J., Laker, R. C., Zhang, M., Kundu, M., and Yan, Z. (2017) Ulk1-mediated autophagy plays an essential role in mitochondrial remodeling and functional regeneration of skeletal muscle. *Am. J. Physiol. Cell Physiol.* **312**, C724–C732
70. Nichenko, A. S., Southern, W. M., Atuan, M., Luan, J., Peissig, K. B., Foltz, S. J., Beedle, A. M., Warren, G. L., and Call, J. A. (2016) Mitochondrial maintenance via autophagy contributes to functional skeletal muscle regeneration and remodeling. *Am. J. Physiol. Cell Physiol.* **311**, C190–C200
71. Durcan, T. M., and Fon, E. A. (2015) The three 'P's of mitophagy: PARKIN, PINK1, and post-translational modifications. *Genes Dev.* **29**, 989–999
72. Wu, H., and Chen, Q. (2015) Hypoxia activation of mitophagy and its role in disease pathogenesis. *Antioxid. Redox Signal.* **22**, 1032–1046
73. Kang, C., Goodman, C. A., Hornberger, T. A., and Ji, L. L. (2015) PGC-1α overexpression by in vivo transfection attenuates mitochondrial deterioration of skeletal muscle caused by immobilization. *FASEB J.* **29**, 4092–4106
74. Kang, C., and Ji, L. L. (2016) PGC-1α overexpression via local transfection attenuates mitophagy pathway in muscle disuse atrophy. *Free Radic. Biol. Med.* **93**, 32–40
75. Liu, J., Peng, Y., Feng, Z., Shi, W., Qu, L., Li, Y., Liu, J., and Long, J. (2014) Reloading functionally ameliorates disuse-induced muscle atrophy by reversing mitochondrial dysfunction, and similar benefits are gained by administering a combination of mitochondrial nutrients. *Free Radic. Biol. Med.* **69**, 116–128
76. Mishra, P., Varuzhanyan, G., Pham, A. H., and Chan, D. C. (2015) Mitochondrial dynamics is a distinguishing feature of skeletal muscle fiber types and regulates organellar compartmentalization. *Cell Metab.* **22**, 1033–1044
77. Sin, J., Andres, A. M., Taylor, D. J., Weston, T., Hiraumi, Y., Stotland, A., Kim, B. J., Huang, C., Doran, K. S., and Gottlieb, R. A. (2016) Mitophagy is required for mitochondrial biogenesis and myogenic differentiation of C2C12 myoblasts. *Autophagy* **12**, 369–380
78. Kim, B., Kim, J. S., Yoon, Y., Santiago, M. C., Brown, M. D., and Park, J. Y. (2013) Inhibition of Drp1-dependent mitochondrial division impairs myogenic differentiation. *Am. J. Physiol. Regul. Integr. Comp. Physiol.* **305**, R927–R938
79. Barbieri, E., Battistelli, M., Casadei, L., Vallorani, L., Piccoli, G., Guescini, M., Gioacchini, A. M., Polidori, E., Zeppa, S., Ceccaroli, P., Stocchi, L., Stocchi, V., and Falcieri, E. (2011) Morphofunctional and biochemical approaches for studying mitochondrial changes during myoblasts differentiation. *J. Aging Res.* **2011**, 845379
80. Koopman, R., Ly, C. H., and Ryall, J. G. (2014) A metabolic link to skeletal muscle wasting and regeneration. *Front. Physiol.* **5**, 32
81. Ceco, E., Weinberg, S. E., Chandel, N. S., and Sznajder, J. I. (2017) Metabolism and skeletal muscle homeostasis in lung disease. *Am. J. Respir. Cell Mol. Biol.* **57**, 28–34
82. Fortini, P., Ferretti, C., Iorio, E., Cagnin, M., Garribba, L., Pietraforte, D., Falchi, M., Pascucci, B., Baccarini, S., Morani, F., Phadngam, S., De Luca, G., Isidoro, C., and Dogliotti, E. (2016) The fine tuning of metabolism, autophagy and differentiation during in vitro myogenesis. *Cell Death Dis.* **7**, e2168
83. Fortini, P., Iorio, E., Dogliotti, E., and Isidoro, C. (2016) Coordinated metabolic changes and modulation of autophagy during myogenesis. *Front. Physiol.* **7**, 237
84. Abreu, P., Mendes, S. V., Ceccatto, V. M., and Hirabara, S. M. (2017) Satellite cell activation induced by aerobic muscle adaptation in response to endurance exercise in humans and rodents. *Life Sci.* **170**, 33–40

Received for publication December 1, 2017.
Accepted for publication July 30, 2018.